

A Near-infrared BODIPY-based Rhomboidal Metallacycle for Imaging-guided Photothermal Therapy

Jinjin Zhang,^{a,†} Jialin Yu,^{a,†} Wen Li,^a Yiqi Fan,^a Yang Li,^a Yan Sun,^b Shouchun Yin^{*a}
and Peter J. Stang^{*b}

^a*College of Material, Chemistry and Chemical Engineering, Key Laboratory of Organosilicon Chemistry and Material Technology, Ministry of Education, Key Laboratory of Organosilicon Material Technology, Hangzhou Normal University, Hangzhou 310036, People's Republic of China*

^b*Department of Chemistry, University of Utah, 315 South 1400 East, Room 2020, Salt Lake City, Utah 84112, United States*

[†]*These authors contributed equally to this work.*

Fax: (+86)57128865077; Tel: (+86)57128865077;

E-mail: yinsc@hznu.edu.cn, and stang@chem.utah.edu

Table of Contents

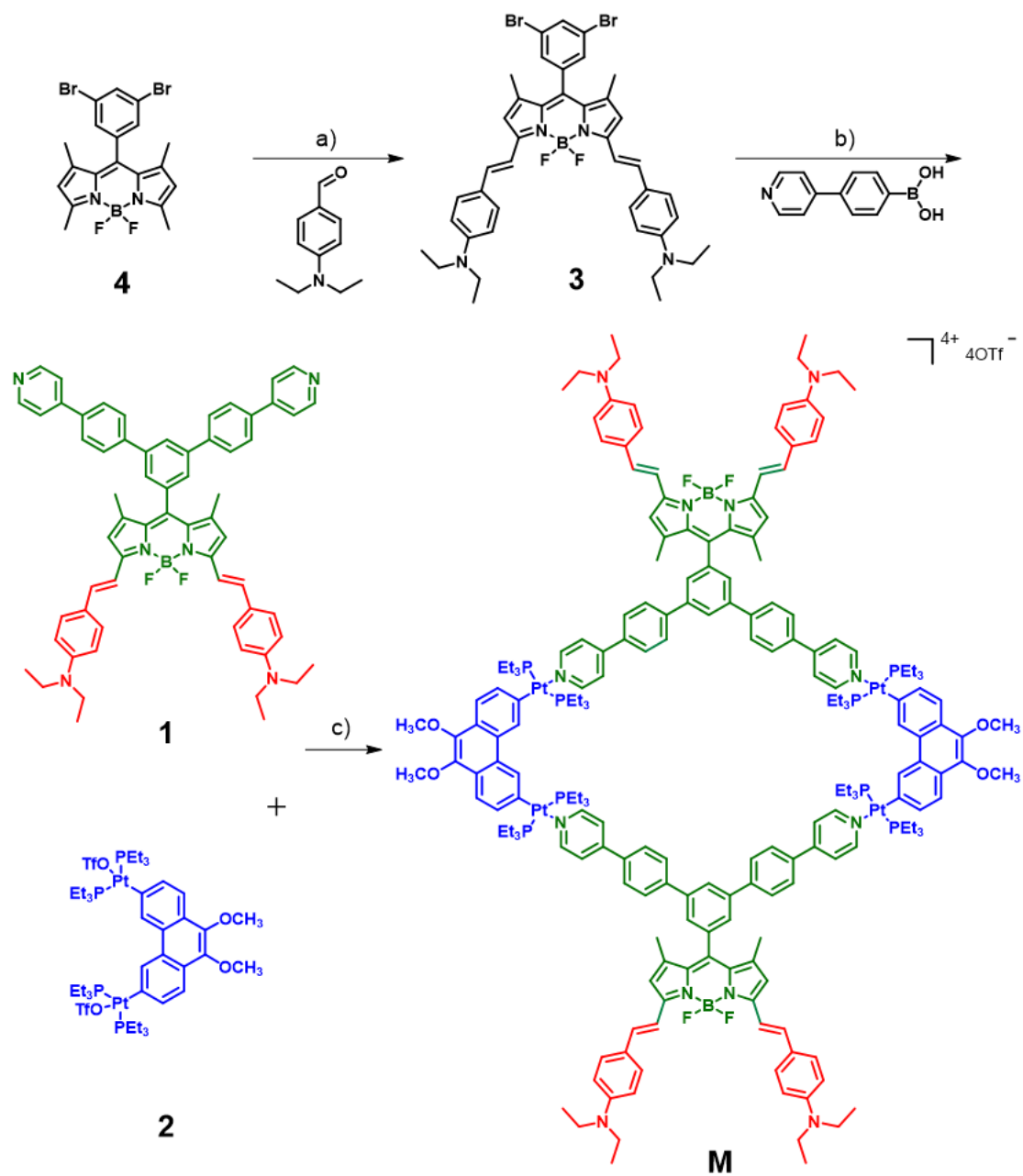
<i>1. Materials and methods</i>	3
<i>2. Synthetic procedures and characterization data</i>	4
<i>2.1 Synthesis of compound 4</i>	5
<i>2.2. Synthesis of compound 3</i>	5
<i>2.3 Synthesis of compound 1</i>	8
<i>2.4. Synthesis of compound 2</i>	11
<i>2.5. Synthesis of M</i>	13
<i>2.6. Fluorescence spectra of compounds</i>	13
<i>3. Preparation of F127/M NPs</i>	16
<i>4. Characterization and properties of F127/M NPs</i>	17
<i>5. Photothermal performance of F127/M NPs</i>	18
<i>6. Evaluation of photostability</i>	19

7. <i>Cell culture</i>	20
8. <i>MTT assay</i>	20
9. <i>Flow cytometer analysis</i>	20
10. <i>Live and dead cell co-staining assay</i>	21
11. <i>Tumor bearing animal model</i>	21
12. <i>In vivo fluorescence imaging</i>	21
13. <i>In vivo antitumor efficacy</i>	22
14. <i>References</i>	22

1. Materials and methods

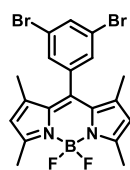
All reagents and deuterated solvents were commercially available and used as supplied without further purification. Compounds **2**^[1] and **4**^[2] were prepared according to the published literature procedures. NMR spectra were recorded on a Bruker Advance 500 MHz spectrometer. ¹H and ¹³C NMR chemical shifts were reported relative to residual solvent signals, and ³¹P{¹H} NMR chemical shifts were referenced to an external unlocked sample of 85% H₃PO₄ ($\delta = 0.0$). Mass spectra were recorded on Micromass Quattro II triple-quadrupole mass spectrometer and 6530 Q-TOF LC/MS. FT-IR spectra were recorded on Bruker VERTEX 70v infrared spectrometer. The UV-vis absorption spectra were measured by a Hitachi U-5300 absorption spectrophotometer. The fluorescent emission spectra were recorded on an Edinburgh FLS 980 fluorescence spectrophotometer, and quantum yields were determined on this equipment using an integral sphere at a concentration of 5 μ M. Transmission electron microscopy (TEM) was performed on a Hitachi F-7700. Dynamic light scattering (DLS) experiments were performed using a Nano ZS90 instrument with a He-Ne laser (633 nm) and 90° collecting optics. MTT method was recorded by microplate reader (Model 550). Flow cytometry (FCM) were observed by Beckman-Coulter. Confocal laser scanning microscope (CLSM) experiments were photographed by Zeiss LSM 510.

2. Synthetic procedures and characterization data



Scheme S1. Synthetic route to **M** and chemical structures of compounds used in this study. Conditions: a) piperidine, *p*-TsOH·H₂O, toluene, 120 °C, reflux, 72 h, 37%; b) Pd(PPh₃)₄, K₂CO₃, THF, H₂O, 60 °C, 12 h, 85%; c) DMSO: MeOH = 1: 1, 50 °C, 12 h, 92%.

2.1 Synthesis of compound 4



Compound **4** was synthesized according to the published procedures^[2]. ¹H NMR (500 MHz, CDCl₃, 298 K) δ (ppm): 7.81 (s, 1H), 7.44 (s, 2H), 6.01 (s, 2H), 2.55 (s, 6H), 1.49 (s, 6H).

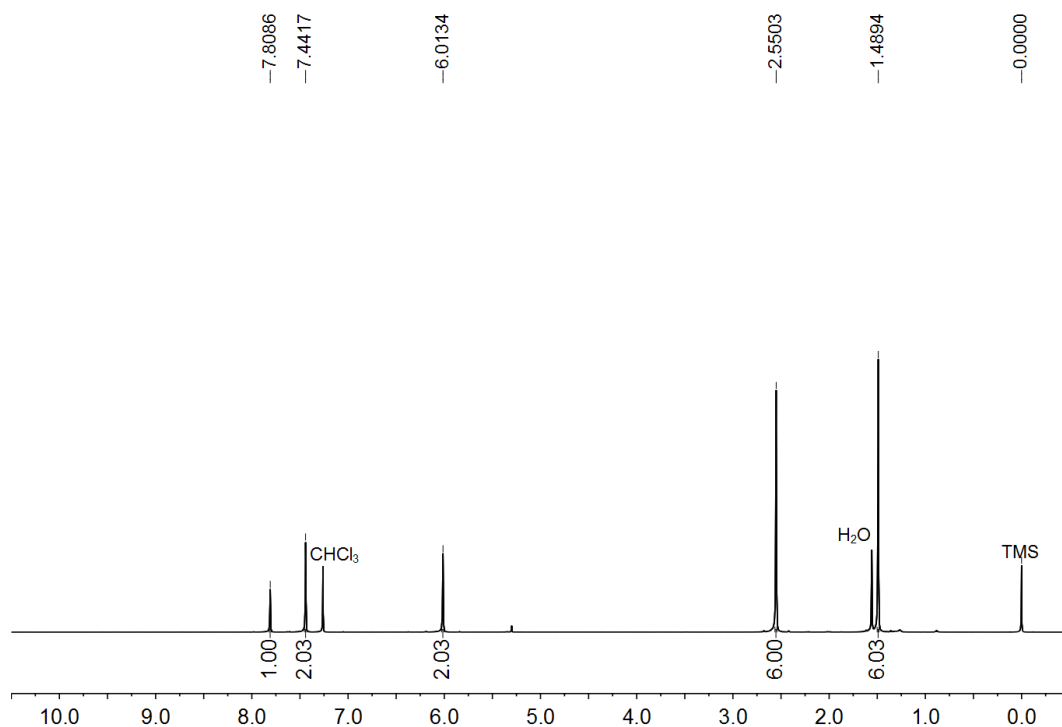
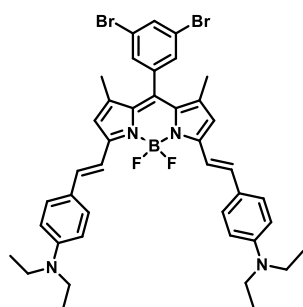


Figure S1. ¹H NMR spectrum (500 MHz, CDCl₃, 298K) recorded for **4**.

2.2. Synthesis of compound 3



Compound **4** (134.0 mg, 0.278 mmol), 4-diethylaminobenzaldehyde (123.0 mg, 0.695 mmol), *p*-TsOH·H₂O (3.0 mg, 0.0158 mmol), piperidine (150 μ L) were dissolved in toluene (6 mL), and the mixture was allowed to react at 120 °C for 72 h. Then the mixture was poured into 100 mL of H₂O, and extracted with CH₂Cl₂ (50 mL \times 3). The organic layers were collected, dried over anhydrous Mg₂SO₄ and concentrated under vacuum. Pure product was obtained via column chromatography (silica gel, 2:1, *v/v*, PE/CH₂Cl₂) as a black solid (82.0 mg, 37%). ¹H NMR (500 MHz, CDCl₃, 298 K) δ (ppm): 7.78 (s, 1H), 7.53–7.47 (m, 6H), 7.47 (s, 2H), 7.21 (s, 1H), 7.17 (s, 1H), 6.66 (d, *J* = 8.5 Hz, 4H), 6.61 (s, 2H), 3.41 (dd, *J* = 13.7, 6.7 Hz, 8H), 1.52 (s, 6H), 1.20 (t, *J* = 6.9 Hz, 12H). ¹³C NMR (126 MHz, CDCl₃, 298 K) δ (ppm): 153.5, 148.6, 140.1,

139.5, 137.2, 134.4, 132.5, 131.4, 131.1, 129.7, 124.3, 123.4, 117.8, 114.3, 111.6, 44.6, 15.3, 12.8. ^{19}F NMR (471 MHz, CDCl_3 , 298 K) δ (ppm): -139.07 (dd, $J = 98.53, 35.09$ Hz, BF_2). ESI-HRMS: m/z 798.1948 [$\mathbf{3} + \text{H}$] $^+$, calcd. for $[\text{C}_{41}\text{H}_{43}\text{BBr}_2\text{F}_2\text{N}_4\text{H}]^+$, 798.2025. FT-IR (cm^{-1}): 3430, 3062, 2966, 2922, 2861, 1589, 1533, 1483, 1363, 1273, 1169, 1107, 1068, 987, 809, 768, 728, 551

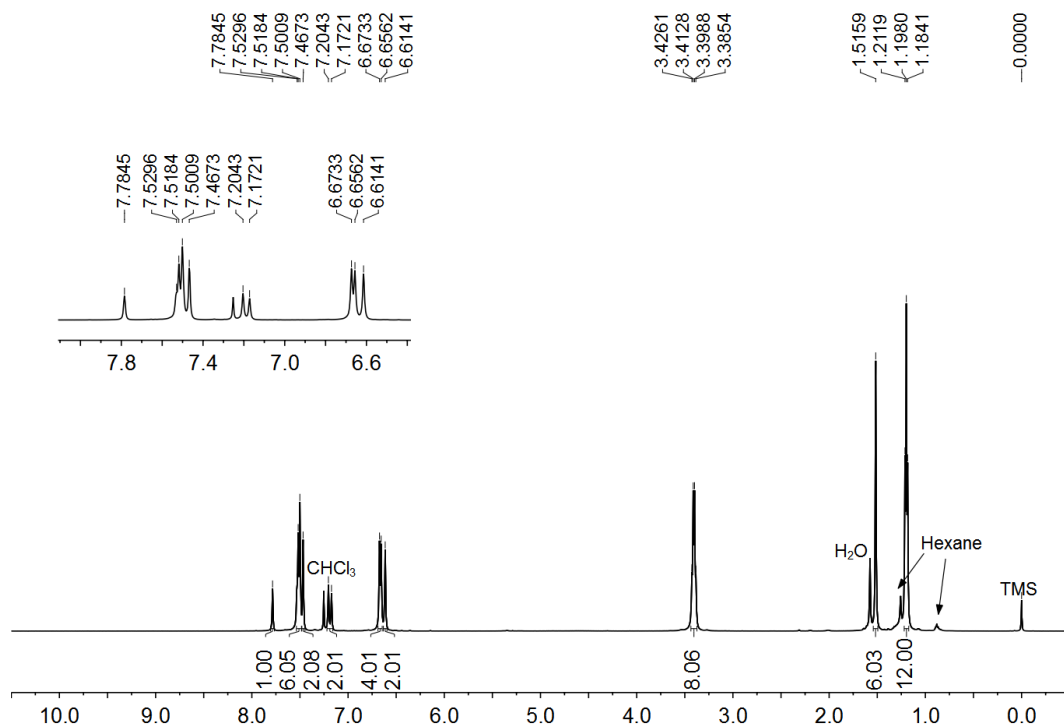


Figure S2. ^1H NMR spectrum (500 MHz, CDCl_3 , 298K) recorded for **3**.

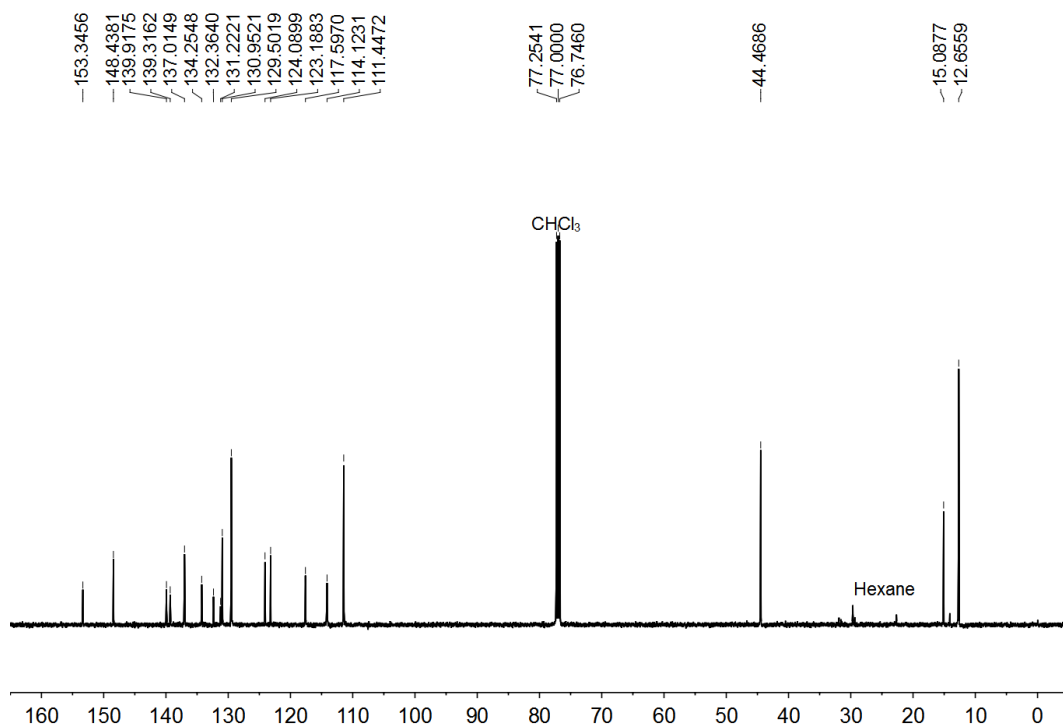


Figure S3. ¹³C NMR spectrum (126 MHz, CDCl₃, 298 K) recorded for **3**.

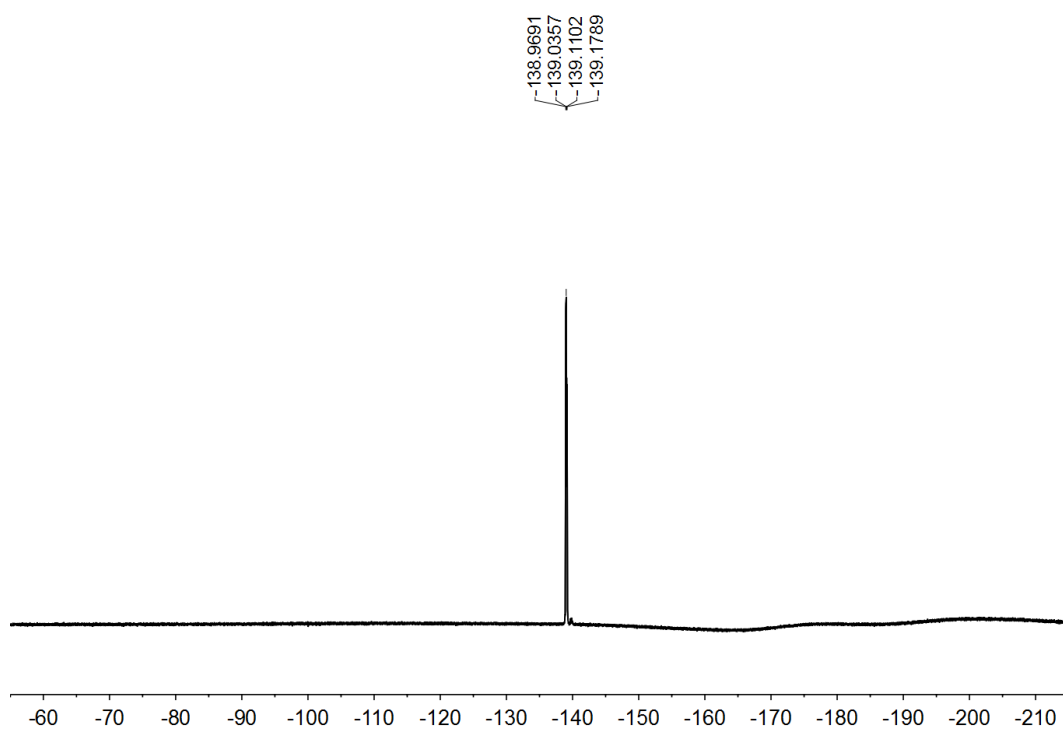


Figure S4. ¹⁹F NMR spectrum (471 MHz, CDCl₃, 298 K) recorded for **3**.

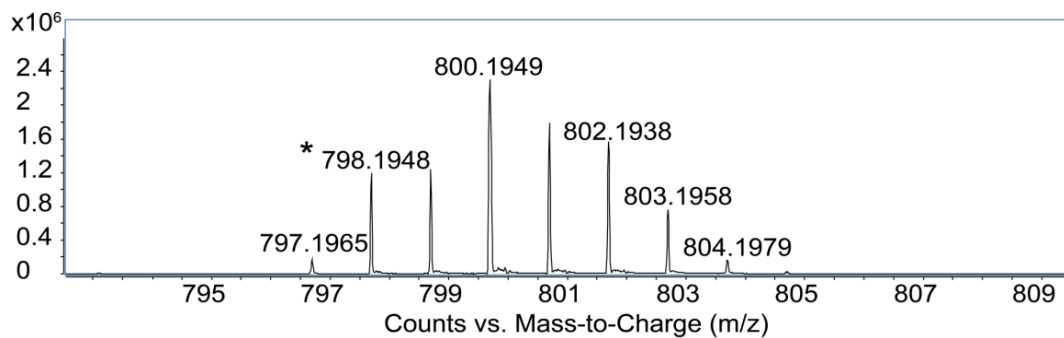


Figure S5. ESI-HRMS spectrum of **3**.

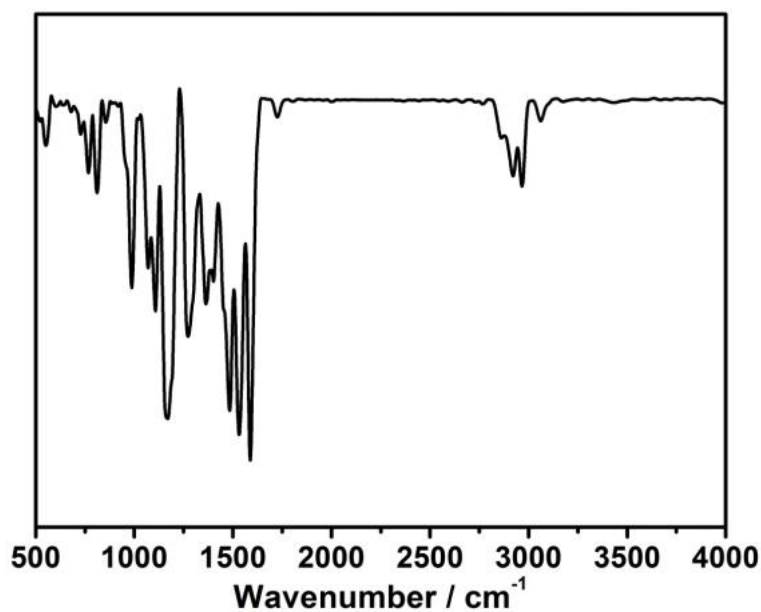
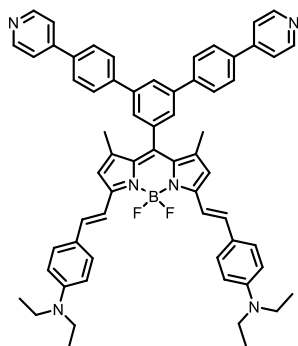


Figure S6 FT-IR spectrum of **3**.

2.3 Synthesis of compound **1**



Compound **3** (100.0 mg, 0.125 mmol), (4-(pyridin-4-yl)phenyl)boronic acid (75.6 mg, 0.374 mmol), K_2CO_3 (68.8 mg, 0.499 mmol) and $Pd(PPh_3)_4$ (14.4 mg, 0.0125 mmol) were added to a 100 mL Schlenk flask containing THF (40 mL) and H_2O (10 mL). The freeze-pump-thaw cycle was performed for three times. The mixture was reacted at 65 °C under nitrogen for 12 h. After that, the reaction mixture was cooled to room temperature, extracted with CH_2Cl_2 (50 mL \times 3), and the solvent was removed by reduced pressure.

The crude product was purified via column chromatography (silica gel, 40:1, v/v, CH₂Cl₂/CH₃OH) to obtain the pure product as a black solid (100.0 mg, 85%). ¹H NMR (500 MHz, CDCl₃, 298 K) δ (ppm): 8.69 (d, *J* = 3.2 Hz, 4H), 8.01 (s, 1H), 7.79 (dd, *J* = 19.8, 8.0 Hz, 8H), 7.63–7.52 (m, 12H), 7.20 (d, *J* = 16.0 Hz, 2H), 6.69 (d, *J* = 7.9 Hz, 4H), 6.61 (s, 2H), 3.42 (d, *J* = 6.7 Hz, 8H), 1.55 (s, 6H), 1.21 (t, *J* = 6.8 Hz, 12H). ¹³C NMR (126 MHz, CDCl₃, 298 K) δ (ppm): 153.0, 150.1, 148.3, 147.5, 141.4, 140.6, 137.5, 137.1, 136.7, 129.4, 127.7, 127.5, 126.6, 125.6, 124.2, 121.5, 117.3, 114.2, 111.5, 44.5, 15.0, 12.6. ¹⁹F NMR (471 MHz, CDCl₃, 298 K) δ (ppm): -138.74 (dd, *J* = 86.52, 40.32 Hz, BF₂). ESI-HRMS: *m/z* 948.4925 [**1** + H]⁺, calcd. for [C₆₃H₅₉BF₂N₆H]⁺, 948.4971. FT-IR (cm⁻¹): 3433, 3033, 2970, 2923, 1590, 1528, 1481, 1404, 1360, 1271, 1168, 1109, 1068, 987, 813, 770, 729.

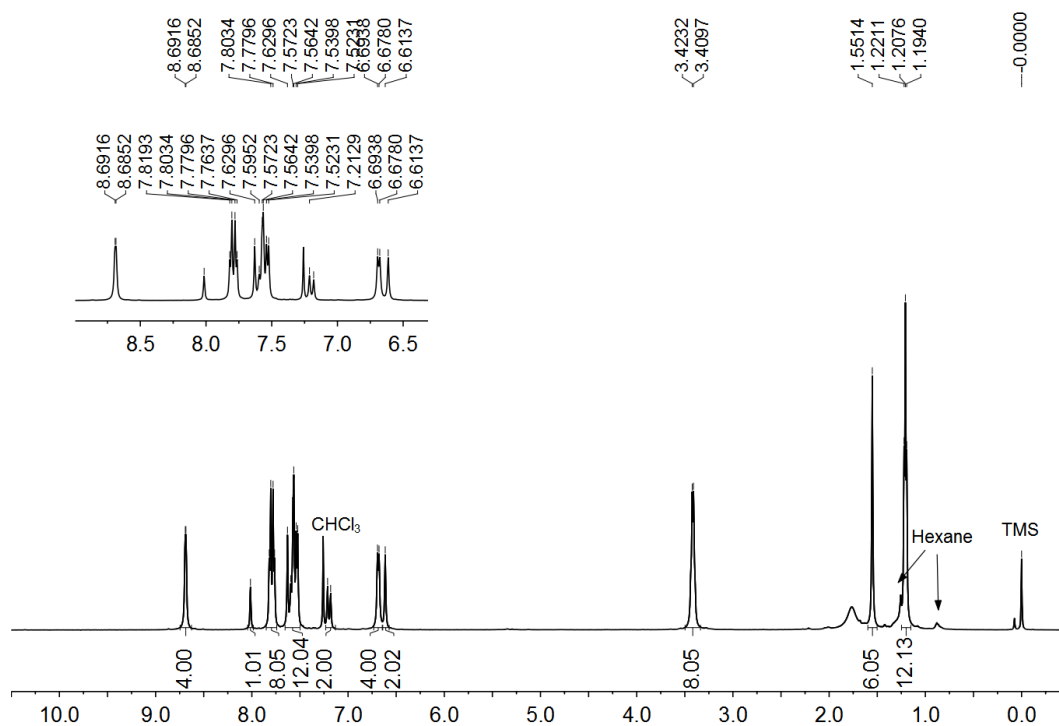


Figure S7. ¹H NMR spectrum (500 MHz, CDCl₃, 298K) recorded for **1**.

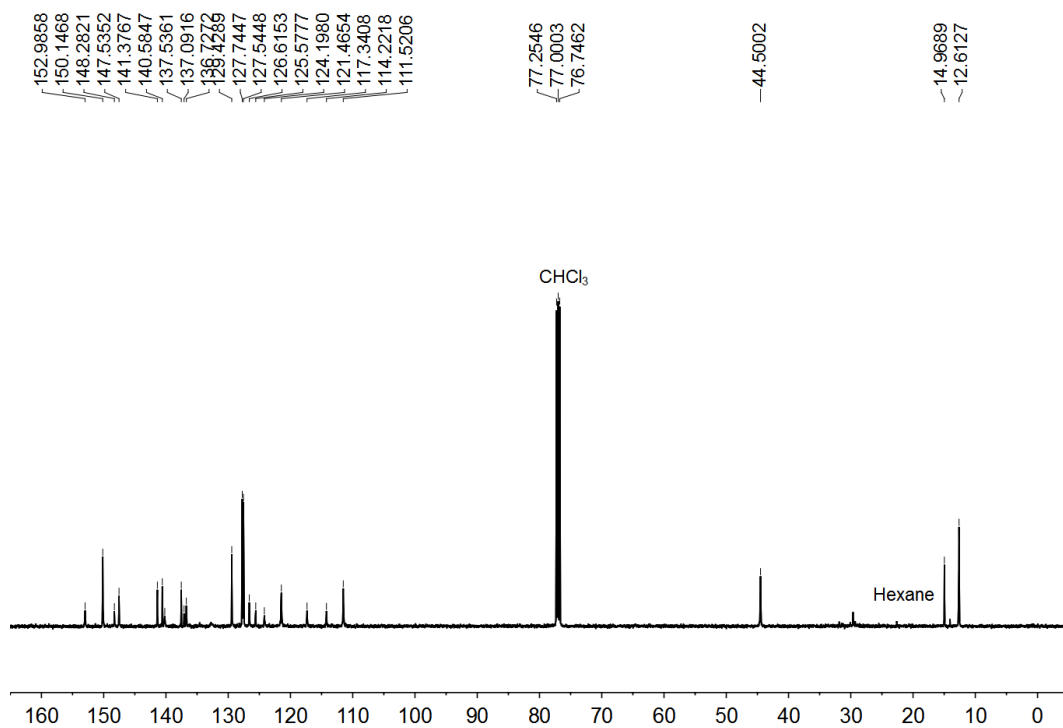


Figure S8. ¹³C NMR spectrum (126 MHz, CDCl₃, 298 K) recorded for **1**.

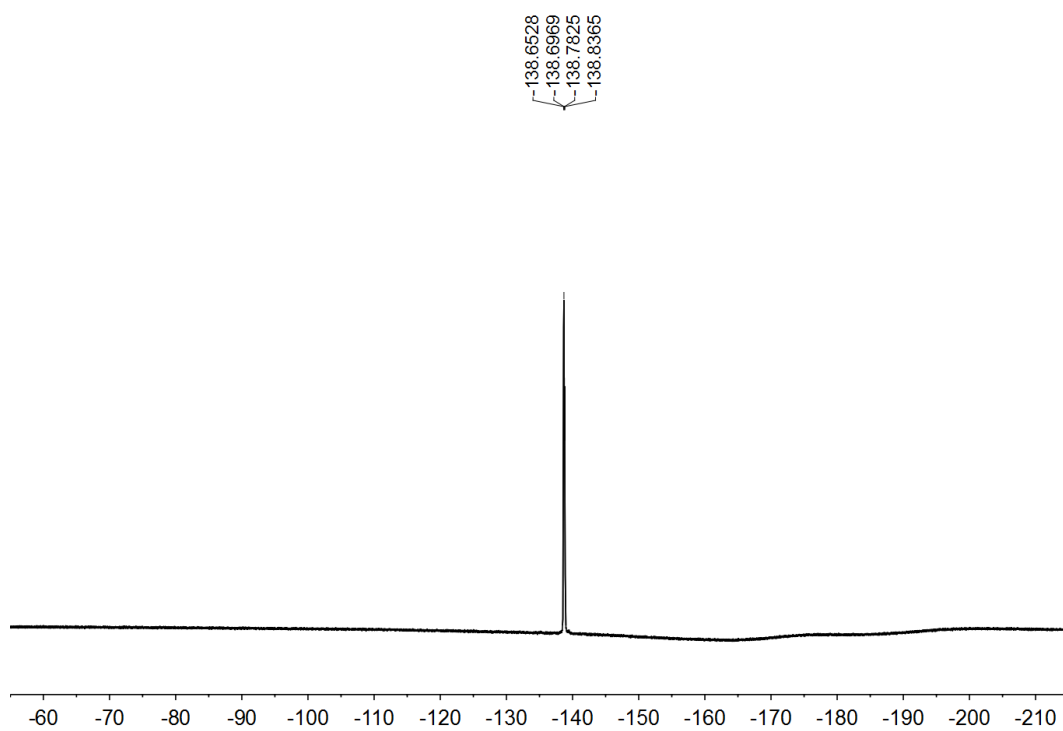


Figure S9. ¹⁹F NMR spectrum (471 MHz, CDCl₃, 298 K) recorded for **1**.

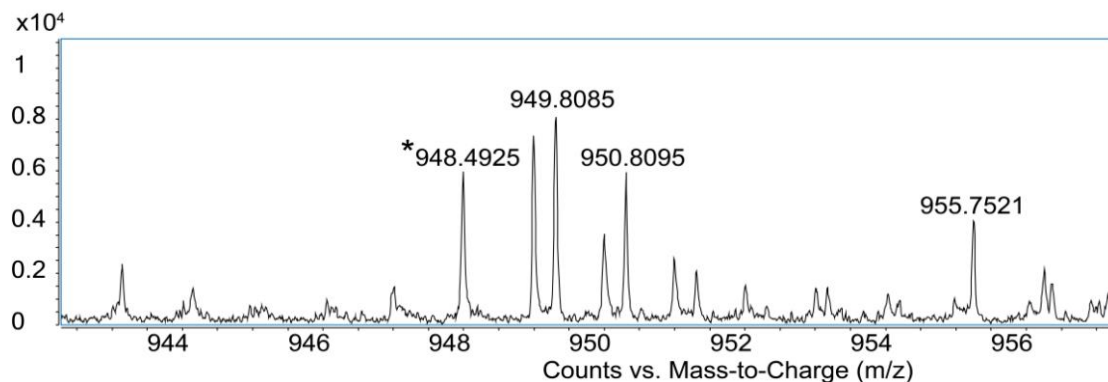


Figure S10. ESI-HRMS spectrum of **1**.

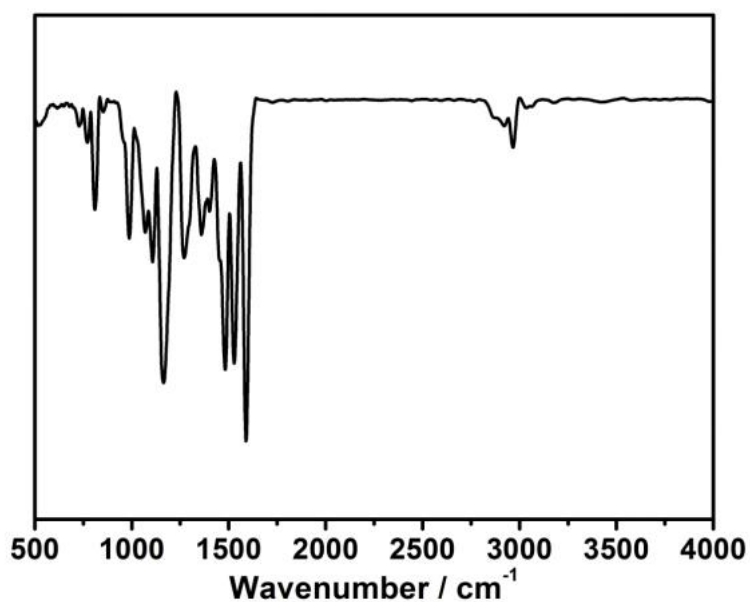
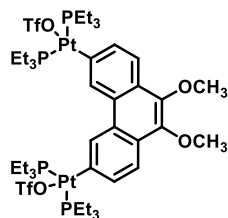


Figure S11 FT-IR spectrum of **1**.

2.4. Synthesis of compound **2**

Compound **2** was synthesized according to the published procedures^[1]. ¹H NMR (500 MHz, CD₂Cl₂, 298 K) δ (ppm): 8.49 (s, 2H), 7.70 (d, $J = 8.2$ Hz, 2H), 7.60 (d, $J = 8.3$ Hz, 2H), 4.03 (s, 6H), 1.69–1.65 (m, 24H), 1.08–1.05 (m, 36H). ³¹P{¹H} NMR (202 MHz, MeOD, 298 K) δ (ppm): 21.59 ppm (s, ¹⁹⁵Pt satellites, ¹ $J_{\text{Pt-P}} = 2782.5$ Hz).



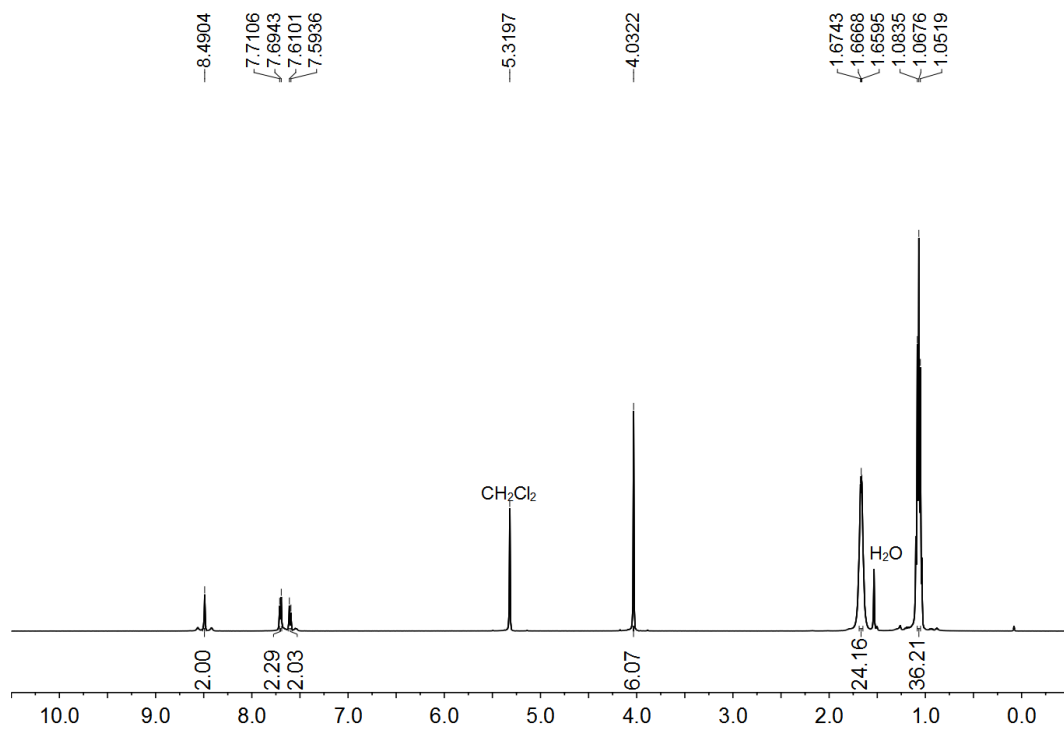


Figure S12. ¹H NMR spectrum (500 MHz, CD₂Cl₂, 298 K) recorded for **2**.

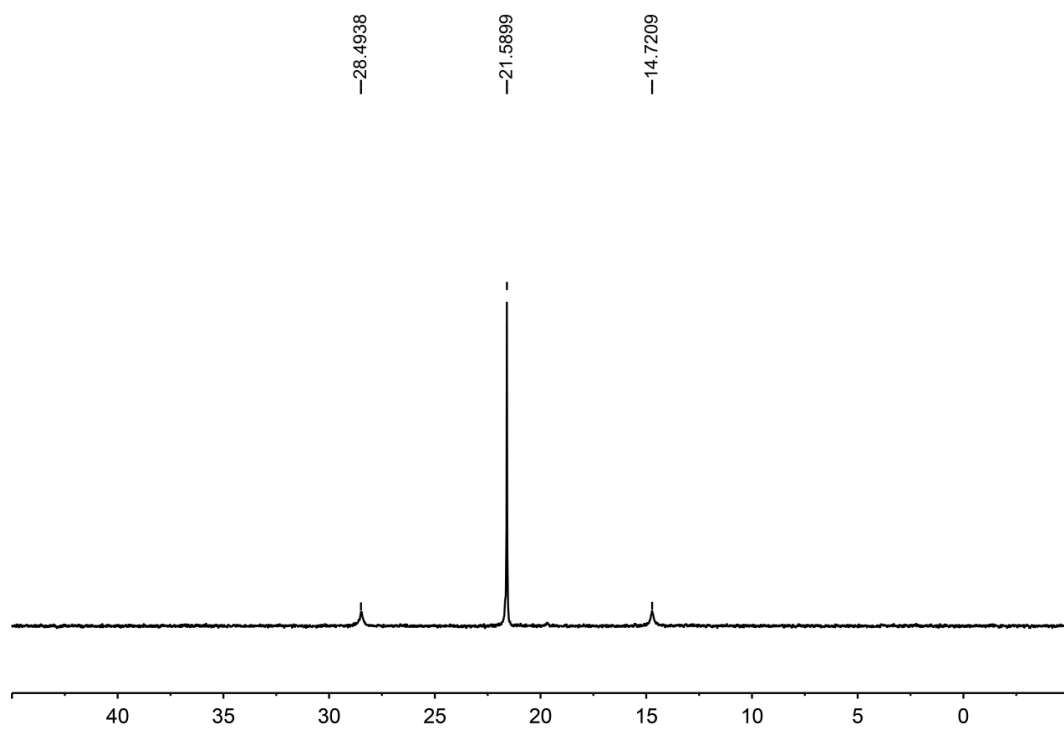


Figure S13. ³¹P{¹H} NMR spectrum (202 MHz, MeOD, 298 K) recorded for **2**.

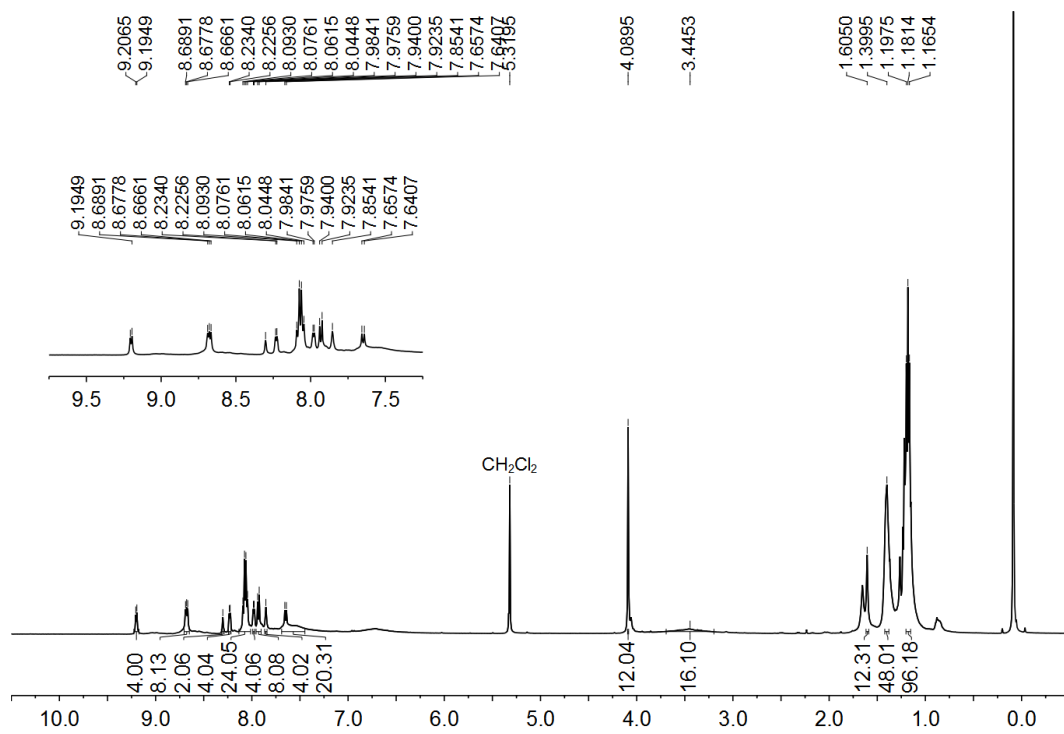


Figure S14. ^1H NMR spectrum (500 MHz, CD_2Cl_2 , 298 K) recorded for **M**.

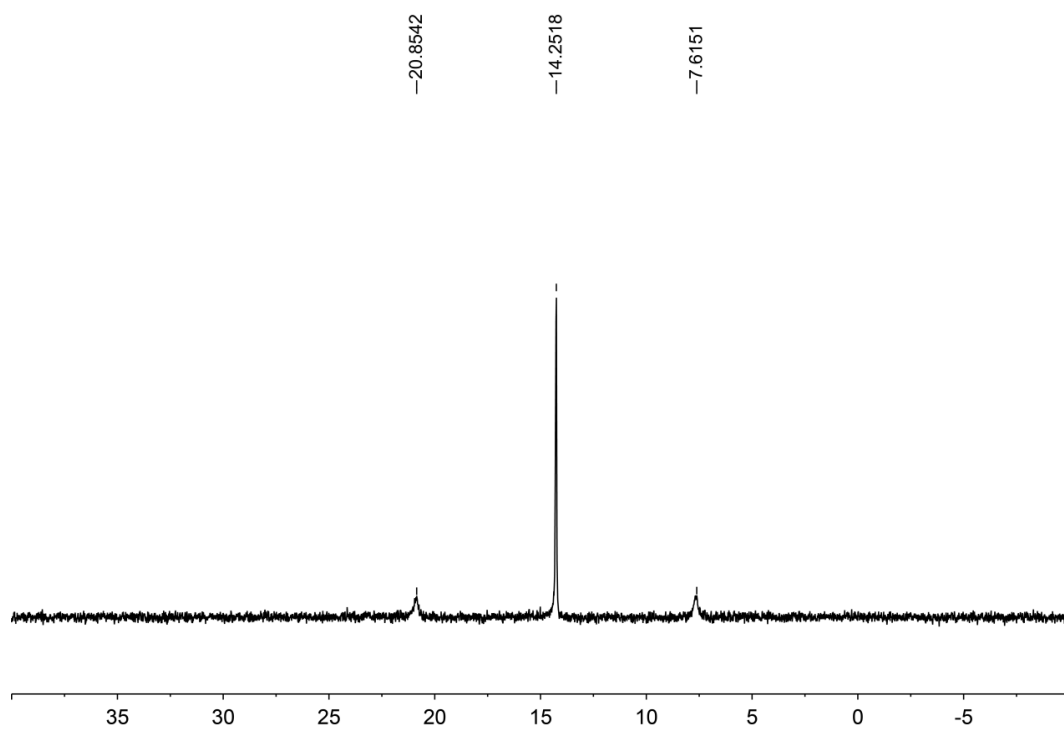


Figure S15. $^{31}\text{P}\{^1\text{H}\}$ NMR spectrum (202 MHz, MeOD, 298 K) recorded for **M**.

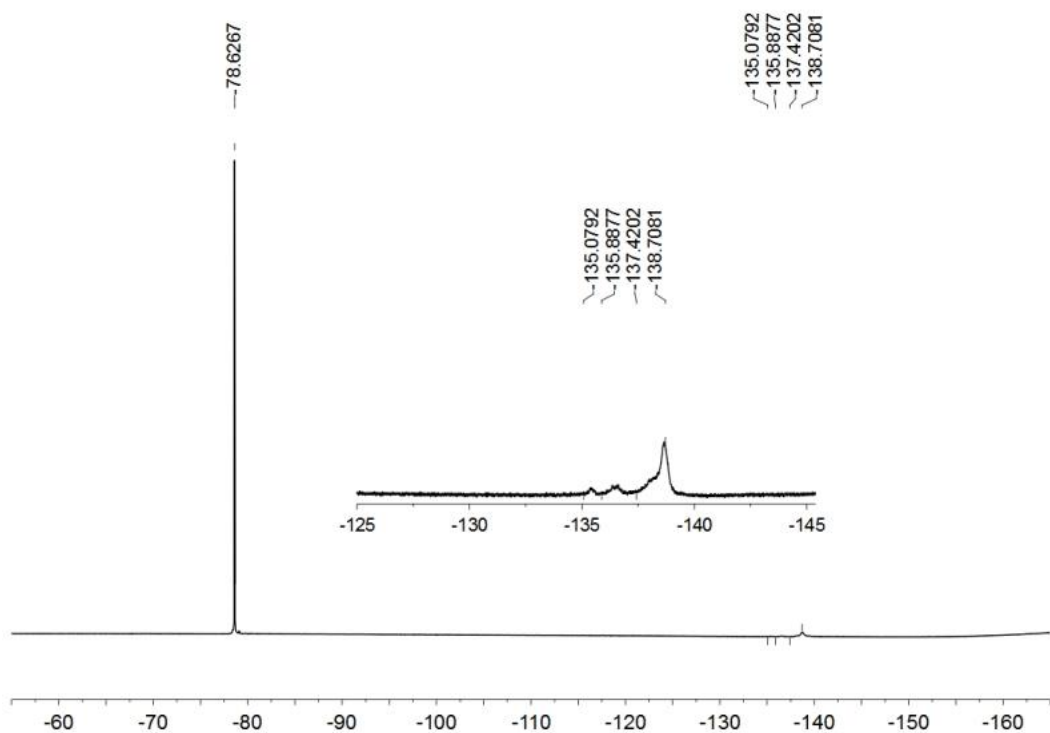


Figure S16. ^{19}F NMR spectrum (471 MHz, CD_2Cl_2 , 298 K) recorded for **M**.

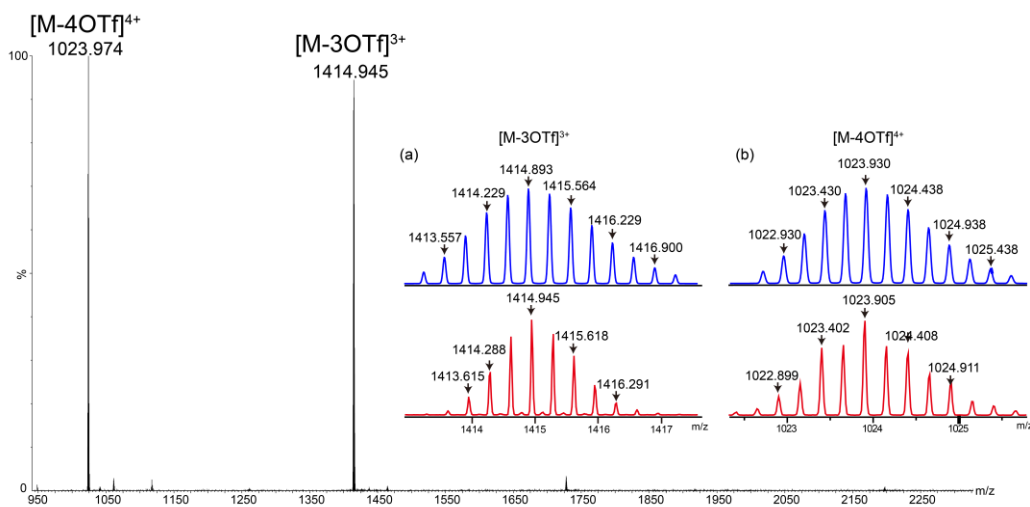


Figure S17. ESI-TOF-MS spectrum of **M**. Experimental (red) and calculated (blue) ESI-TOF-MS spectra of **1**: (a) $[\text{M} - 4\text{OTf}]^{4+}$ and (b) $[\text{M} - 3\text{OTf}]^{3+}$.

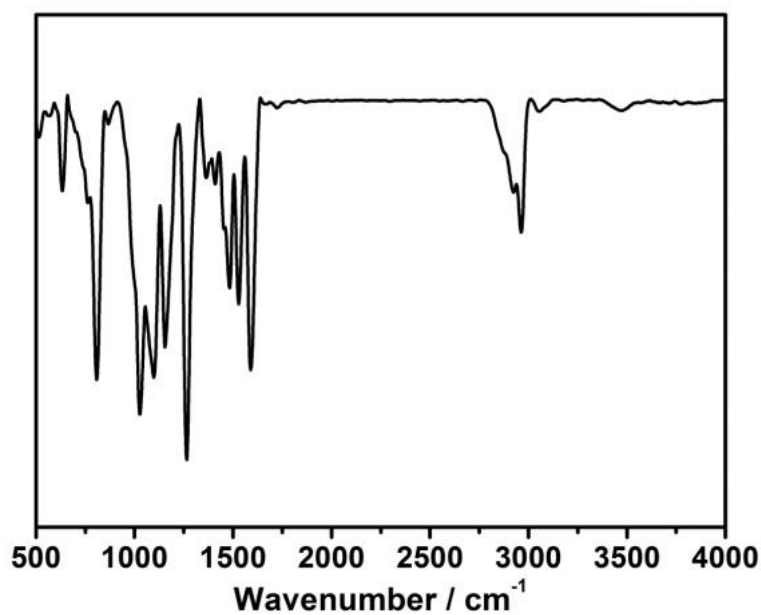


Figure S18. FT-IR spectrum of **M**.

2.6. Fluorescence spectra of compounds

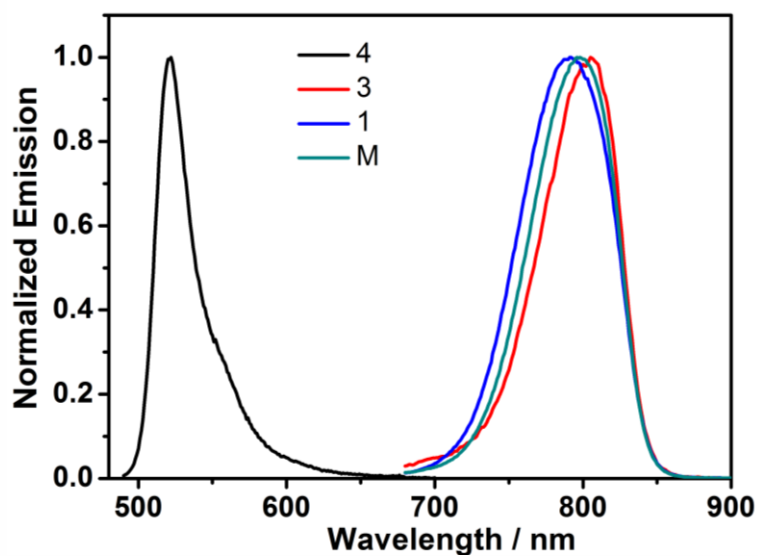


Figure S19 Normalized fluorescence spectra of **1**, **3**, **4** and **M** in DMSO.

3. Preparation of F127/**M** NPs

The NPs were prepared *via* the precipitation method. **M** (2.0 mg) was dissolved in acetone (1 mL). The **M** solution (2 mg/mL) was then slowly dropped into a F127 aqueous solution (10.0 mg F127 in 10 mL water) under stirring at room temperature. The mixture kept stirring in the fume hood overnight to vaporize the acetone. The

aqueous solution was then further filtered through a 0.45 μm filter to obtain a clear brown solution.

4. Characterization and properties of F127/M NPs

Dynamic light scattering (DLS). For particle size measurement, the solution of F127/M NPs was diluted with deionized water and passed through a 0.45 μm filter. Using Nano ZS90 instrument with a He-Ne laser (633 nm) and 90° collecting optics at 25 °C.

Transmission electron microscopy (TEM). Diluted aqueous solution of F127/M NPs (15 μL) was dropped to a 200-mesh carbon coated copper grid and air-dried for 3 days. TEM observations were conducted on a Hitachi F-7700.

Stability studies of F127/M NPs. The particle size of the obtained F127/M NPs solutions as-prepared and after 3 weeks were measured by DLS to verify stability *in vitro*.

Drug loading efficiency: Concentration-dependent absorbance of **M** was drawn and the absorbance at 715 nm could make a linear fitting to the concentration of **M**. The drug loading efficiency (DL%) and encapsulation efficiency (EE%) of **M** were calculated by the following two equations:

$$\text{EE}\% = \frac{\text{Weight of the agent in micelles}}{\text{Weight of the feeding agent}} \times 100\%$$

$$\text{DL}\% = \frac{\text{Weight of the agent in micelles}}{\text{Weight of the feeding F127 and agent}} \times 100\%$$

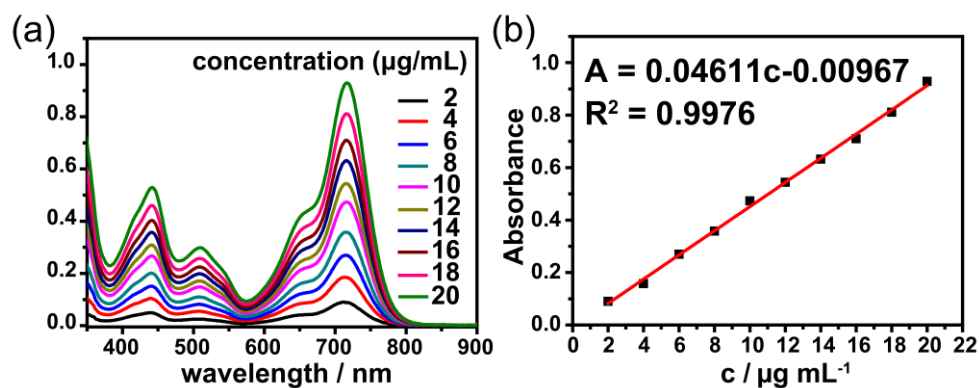


Figure S20. (a) Concentration-dependent absorbance and (b) the standard curve of **M** in acetone.

5. Photothermal performance of F127/M NPs

Upon the irradiation, the temperature of the F127/M NPs aqueous solution was measured every 60 s. 1.0 mL of F127/M NPs aqueous solution (20 μM) was first irradiated with a 660 nm laser continually with different power density (0.3, 0.7, 1.0, 1.5, 1.8 W/cm^2), respectively. Then, 1.0 mL of F127/M NPs aqueous solution with different concentration (0, 5, 10, 15, 20 μM) was exposed to 660 nm laser (1.0 W/cm^2), respectively. To evaluate the photothermal stability, the temperature changes of the F127/M NPs aqueous solution (10 μM) during five cycles of 660 nm laser irradiation (1.0 W/cm^2 ; 10 min per cycle) were recorded. The photothermal conversion efficiency (PCE) was calculated as the methods reported in the literature^[3]. Briefly, 1.0 mL of the F127/M NPs aqueous solution (20 μM) was irradiated with a 660 nm laser (1.8 W/cm^2) continually in 10 min, and then naturally cooling down to the room temperature in 20 min. In the meantime, the water was used as a control group. PCE was calculated according to the following Equation (1):

$$\text{PCE} = \frac{hS(T_{max} - T_{surr}) - Q_{dis}}{I(1 - 10^{-A_{660}})} \dots \dots (1)$$

where h is the heat transfer coefficient, S is the surface area of the container, T_{max} and T_{surr} are the maximum temperature and surrounding temperature, respectively. Q_{dis} represents heat dissipated from the laser mediated by the solvent and container. I is the laser power and A is the absorbance of the F127/M NPs aqueous at 660 nm. Q_{dis} is the heat dissipation by the solvent and is calculated from equation (2):

$$Q_{dis} = \frac{mC(T_{max,water} - T_{surr})}{\tau_{water}} \dots \dots (2)$$

Where m and C are the mass and heat capacity of water, $T_{max,water}$ is the maximum temperature of water, T_{surr} is the surrounding temperature of environment, and τ_{water} is the associated time constant for solvent water. The value of hS is determined from equation (3):

$$hS = \frac{mC}{\tau} \dots \dots (3)$$

where m and C are the mass and heat capacity of water, and τ is the associated time constant determined by equation (4):

$$t = -\tau \ln \theta = -\tau \ln \left(\frac{T_{surr} - T}{T_{surr} - T_{max}} \right) \dots \dots (4)$$

where t is the cooling time and θ is a dimensionless parameter representing the driving force of the temperature. T_{surr} is the surrounding temperature of environment, T is the temperature of the F127/M NPs aqueous solution over time, T_{max} is the maximum temperature of the F127/M NPs aqueous solution. The value of τ can be obtained by equation.

6. Evaluation of photostability

Aqueous solution of F127/M NPs or ICG (10 μ M) are exposed to 660 nm (1.0 W/cm²) laser, respectively. The UV-vis absorption spectra were recorded at 1 min intervals to evaluate photostability. Furthermore, ³¹P{¹H} NMR spectra of M before and after irradiation (660 nm, 1.0 W/cm², 10 min) were also used to verify photostability.

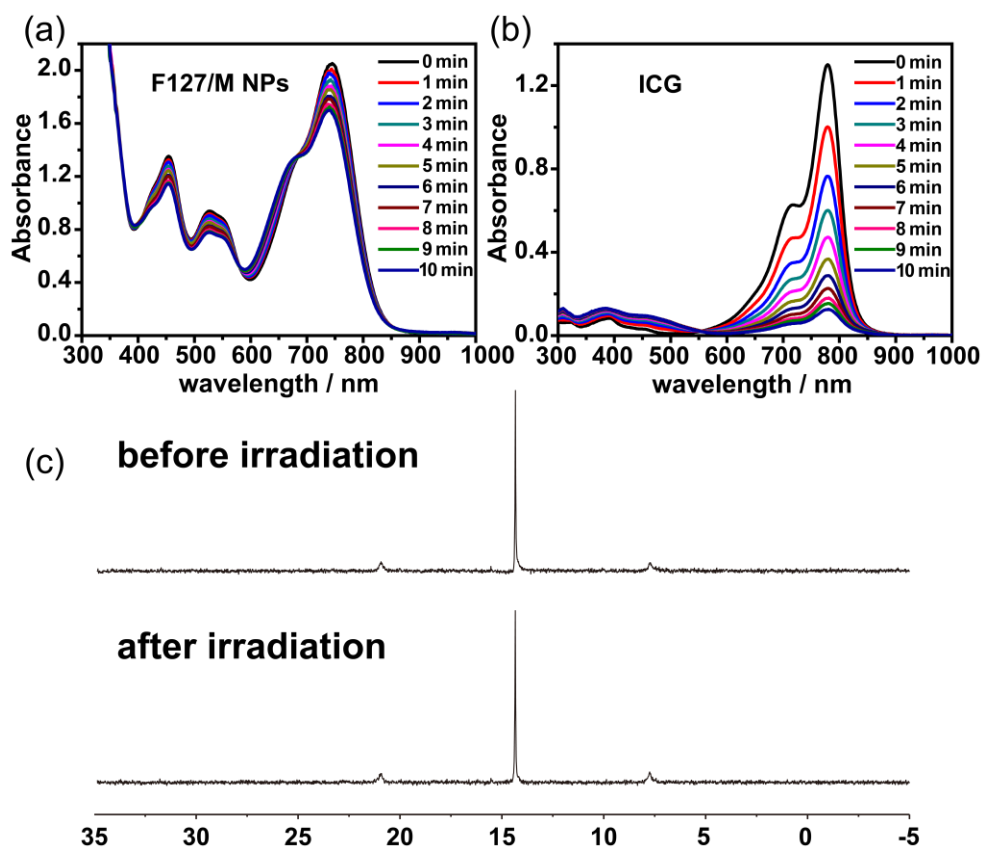


Figure S21. UV-vis absorption spectra of (a) F127/M NPs, (b) ICG with different irradiation time (660 nm, 1.0 W/cm²). (c) ³¹P{¹H} NMR spectra of M before and after irradiation (660 nm, 1.0 W/cm², 10 min).

7. Cell culture

U87 cells were cultured in Dulbecco's Modified Eagle Medium (DMEM) containing 10 % fetal bovine serum (FBS) in a humidified atmosphere incubator with 5% CO₂ at 37 °C.

8. MTT assay

U87 cells were cultured in a 96-well plates (1×10^4 cells/well) for 18 h. Various concentrations (0, 1, 2, 4, 6, 8, 10 and 20 $\mu\text{g/mL}$) of F127/M NPs in cell culture media were added into the wells. The cells were divided into a laser group (660 nm, 1.0 W/cm², 5 min) and a non-laser group. After 4 h incubation, the laser group was irradiated with laser, and the non-laser group was kept in the dark as control. After further incubating for 20 h, MTT (0.5 mg/mL, 100 μL) was added into the wells and incubated for another 4 h. Then DMSO (100 μL) was added after removing the medium to dissolve the formazan crystals. Finally, the optical density (OD) was recorded at 570 nm on the microplate reader (Model 550). The normal medium was used as 100% positive control, and the water medium was used as 0% negative control. Each concentration had 6 replicate wells and the experiment was repeated three times. The cell viability (%) was calculated by the following formula:

$$CV (\%) = \frac{[A]_{\text{experimental}} - [A]_{\text{negative}}}{[A]_{\text{positive}} - [A]_{\text{negative}}} \times 100\% \dots \dots (6)$$

Where $[A]_{\text{experiment}}$ is the absorbance of the experimental group, $[A]_{\text{positive}}$ is the absorbance of 100% positive control, and $[A]_{\text{negative}}$ is the absorbance of 0% negative control.

9. Flow cytometer analysis

U87 cells were seeded in 6-well plates and incubated for 18 h. After removing the medium, cells were divided into four groups: 1) control group (without any treatment), 2) laser irradiation group, only laser (660 nm, 1.0 W/cm², 15 min), 3) F127/M NPs group (stained for 30 min), 4) F127/M NPs + laser irradiation group, incubated with F127/M NPs for 30 minutes, and then irradiated upon laser (660 nm, 1.0 W/cm²) for 5

min. After a series of treatments, the cells continued to be cultured for 2 h at 37 °C. The cells were then washed with PBS, digested by trypsinization and collected by centrifuge. Fluorescence intensities were compared by flow cytometry.

10. Live and dead cell co-staining assay

U87 cells were seeded in 6-well plates and incubated for 18 h, and the cells were also divided into the above four groups. After a series of treatments, the cells were continuously cultured for 2 h at 37 °C. The cells were then washed with PBS. Calcein-AM/PI Double Stain Kit were used to stain the cells and CLSM was used to photograph the live and dead cells.

11. Tumor bearing animal model

Female BALB/c nude mice (6 weeks old, weighting about 16-18 g) were purchased from Charles River Laboratory China Branch (Zhejiang, China) with production license number SCXK (Zhejiang) 2019-0001 and certificate number 20211228Abzz0619072327. The mice were housed at the Laboratory Animal Center of Hangzhou Normal University with use license number SYXK (Zhejiang) 2020-0026, and cultivated in a pathogen-free environment with appropriate humidity and temperature. All animal procedures were performed in accordance with the animal care and use guidelines of the Organizational Animal Care and Use Committee. Tumor-bearing mice were prepared by injecting nude mice with 100 μ L of 10^6 U87 single cell suspension in PBS. After 6 days, F127/**M** NPs was injected intratumorally into U87 tumor mice with an average volume of approximately 120 mm³ to evaluate the therapeutic effect.

12. In vivo fluorescence imaging

Nude mice were also anesthetized and injected intratumorally with F127/**M** NPs as described above. Among them, fluorescence imaging was performed at different time points (1, 4, 8, 16, 24 h) by small animal imaging system using a 662 nm excitation filter and a 697 nm emission filter, respectively. Major organs (heart, live, spleen, lung,

and kidney) were excised from sacrificed mice and fluorescent images were obtained.

13. *In vivo antitumor efficacy*

U87 tumor-bearing mice were randomly divided into 4 groups when tumors grew to $\sim 120 \text{ mm}^3$ ($n = 6$). I): PBS group (only 200 μL), II): PBS + Laser group, PBS (200 μL) + 660 nm laser (1.0 W/cm^2 , 5 min), III): F127/M NPs group (only 200 μL , 200 $\mu\text{g/mL}$), IV): F127/M NPs + Laser group, F127/M NPs (200 μL , 200 $\mu\text{g/mL}$) + 660 nm (1.0 W/cm^2 , 5 min). The body weight and tumor volume of mice were monitored every two days.

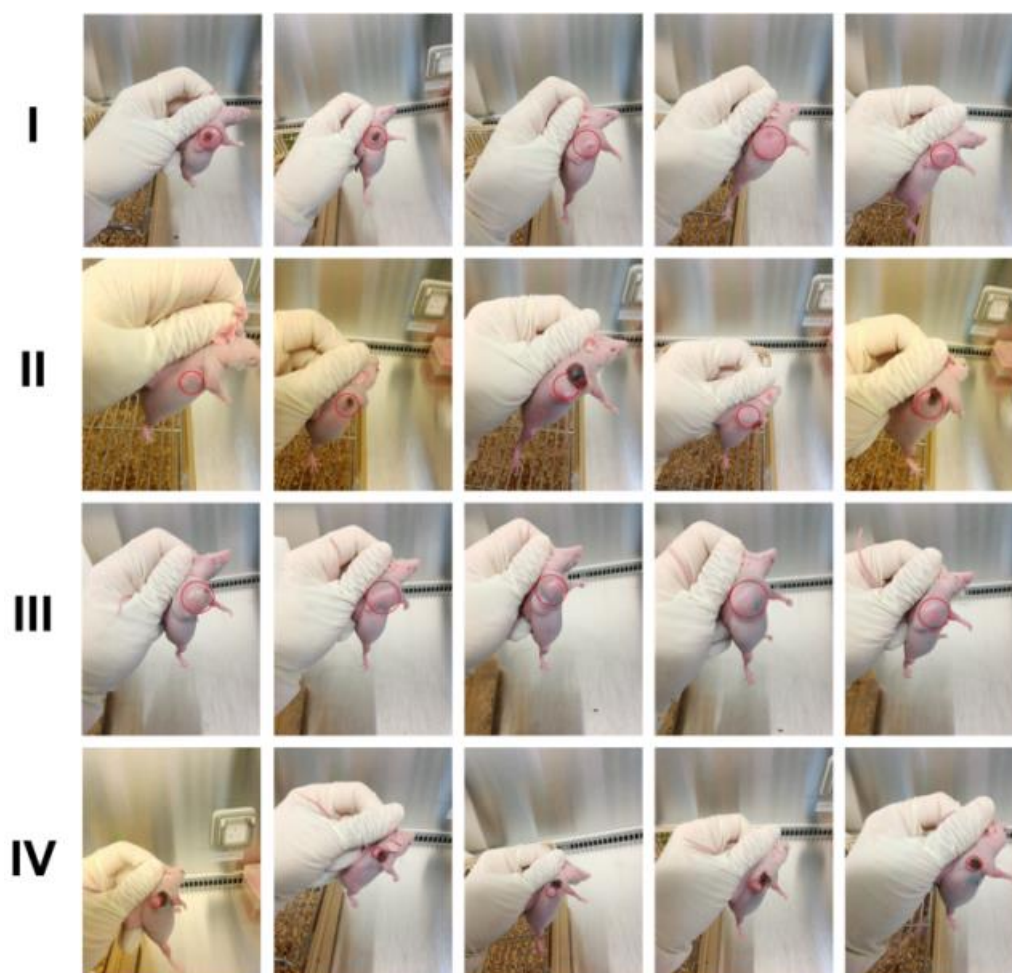


Figure S22. The photos of U87 tumor-bearing nude mice after 14 days in different treatment groups.

14. *References*

[1] Y. Li, X. C. Yuan, J. L. Yu, Y. Fan, T. He, S. Lu, X. Li, H. Qiu, S. Yin, Amphiphilic

rhomboidal organoplatinum(II) metallacycles with encapsulated doxorubicin for synergistic cancer therapy [J]. *ACS Appl. Bio Mater.* **2020**, *3*, 8061–8068.

[2] W. Sun, R. Chen, X. J. Cheng, L. Marin, Bodipy-based chemosensors for highly sensitive and selective detection of Hg²⁺ ions [J]. *New J. Chem.* **2018**, *42*, 19224–19231.

[3] M. H. Su, Q. J. Han, X. S. Yan, Y. Liu, P. Luo, W. Zhai, Q. Zhang, L. Li, C. Li, A supramolecular strategy to engineering a non-photobleaching and near-infrared absorbing nano-J-aggregate for efficient photothermal therapy [J]. *ACS Nano.* **2021**, *15*, 5032–5042.